

# Monte Carlo simulations of ion selectivity in a biological Na channel: Charge–space competition

Dezső Boda,<sup>a</sup> David D. Busath,<sup>b</sup> Bob Eisenberg,<sup>c</sup> Douglas Henderson<sup>d</sup> and Wolfgang Nonner<sup>\*e</sup>

<sup>a</sup> Department of Physical Chemistry, University of Veszprém, H-8201 Veszprém, P.O. Box 158, Hungary. E-mail: boda@almos.vein.hu

<sup>b</sup> Department of Zoology and Center for Neuroscience, Brigham Young University, Provo, Utah 84602. E-mail: david\_busath@byu.edu

<sup>c</sup> Department of Molecular Biophysics and Physiology, Rush Medical College, Chicago, Illinois 60612. E-mail: beisenbe@rush.edu

<sup>d</sup> Department of Chemistry and Biochemistry, Brigham Young University, Provo, Utah 84602. E-mail: doug@huey.byu.edu

<sup>e</sup> Department of Physiology and Biophysics, University of Miami School of Medicine, University of Miami School of Medicine, Miami, Florida 33101. E-mail: wnonner@chroma.med.miami.edu

Received 16th April 2002, Accepted 2nd September 2002

First published as an Advance Article on the web 18th September 2002

Na channels that produce the action potentials of nerve and muscle include a selectivity filter formed by both positively and negatively charged amino acid residues in a molecular pore. Here we present Monte Carlo simulations of equilibrium ion absorption in such a system. Ions are treated as charged hard spheres in a uniform dielectric. Tethered carboxylate and amino groups known to line the selectivity filter of the Na channel are represented as charged hard spheres and restricted to the filter region of the channel. Consistent with experiments, we find (1) that absorption of  $\text{Ca}^{2+}$  into the filter exceeds absorption of  $\text{Na}^+$  only when the concentration of  $\text{Ca}^{2+}$  is some tenfold larger than physiological; (2) the model channel absorbs smaller alkali metal ions preferentially compared to larger ones. The alkali metal selectivity involves volume exclusion of larger ions from the center of the filter region.

## 1 Introduction

Ion channels are a major class of proteins that bridge cell membranes and thereby control many biological functions in health<sup>1</sup> and disease.<sup>2</sup> Ion channels regulate the flux of ions into the cell and, when open, select between ions. The flux is driven by the gradient of electrochemical potential, and controlled by the physical properties of the channel protein.<sup>3</sup> How proteins control selectivity has long been a central question in biology. Here we examine a mechanism of ion selectivity for the Na channels of nerve and muscle membranes.

Na channels are part of a large family of structurally related voltage-controlled channels that also includes Ca and K channels. The conductive pore in this family is formed between four monomers (K channels) or four homologous motifs within a single polypeptide (Na and Ca channels). The ion-selective properties of the channels seem to arise in small segments of the sequence (the ‘P loop’); these segments form inserts that locally restrict the diameter of a wider pore.<sup>4,5</sup> Site-directed mutations suggest that the constriction in Na- and Ca-specific channels is lined by the sidechains of the amino acid residues, whereas in K channels it is lined by atoms of the polypeptide backbone.<sup>4,6–9</sup>

Ionic selectivities of Na and Ca channels seem largely to be determined by four residues present in corresponding positions of the four P loops. These are all glutamate (E) in Ca channels (the ‘EEEE-locus’), but include aspartate (D), glutamate, lysine (K), and alanine (A) in Na channels (‘DEKA-locus’). Mutating the amino acids in these four positions of the Na channel from DEKA to DEEE produces a strong shift of

selectivity from  $\text{Na}^+$  to  $\text{Ca}^{2+}$ , in effect creating a Ca channel.<sup>10</sup> Further mutagenesis experiments have shown that a positively charged residue in the locus (such as lysine, arginine, or histidine at pH 6) is needed to create the low divalent affinity seen in Na channels.<sup>11,12</sup>

Although crystallographic coordinates of Na channels have not yet been determined, many structural properties of the pore have been deduced by other means. Hille probed the ionic pathway with protons, alkali metal cations, and organic cations, and postulated a structure for the ‘selectivity filter’ of the Na channel.<sup>13,14</sup> In this view, the selective portion is a short axial subsegment of the pore that forms a rectangular frame (aperture  $\approx 0.3 \text{ nm} \times 0.5 \text{ nm}$ ) of oxygen atoms around the ionic pathway, some with charge. It is gratifying that this structural hypothesis, developed 30 years ago, seems consistent with possible arrangements of the actual primary structure, namely the DEKA locus, which was unknown and unguessed at that time, but the physical principles by which the DEKA locus produces the observed alkali metal and alkali earth selectivities remain unknown.

Recently, the physical basis of ionic selectivity in the analogous EEEE locus of Ca channels has been examined using statistical mechanics and a simple model to capture electrostatic and excluded-volume effects in the locus.<sup>15–20</sup> The model is a modest extension and reworking of the standard models of concentrated salt solutions found in the literature of physical chemistry in the last decade or two.<sup>21</sup> The four carboxylate groups in the Ca channel are represented by a cluster of 8 half-charged oxygen ions confined to a small volume (the selectivity filter) but free to move within that volume.

$\text{Ca}^{2+}$  accumulates in preference to  $\text{Na}^+$  or other alkali metal cations (in agreement with experiments on biological Ca channels) because of Coulombic and hard-sphere interactions among these confined oxygens and mobile ions.  $\text{Ca}^{2+}$  is preferred over  $\text{Na}^+$  because one divalent  $\text{Ca}^{2+}$  provides the same amount of charge as two  $\text{Na}^+$  in about one half the ionic volume. The crowding of charge produces selectivity because of the competition of the counterions for space, the charge-space competition (CSC) mechanism.<sup>15,17</sup>

This paper examines how well a CSC mechanism can account for selectivity in the DEKA locus of Na channels. We report Monte Carlo (MC) simulations of the equilibrium ion absorption that arises when  $\text{Na}^+$  ions, other alkali metal cations, and  $\text{Ca}^{2+}$  compete in a simple representation of the DEKA locus.

## 2 Model

The cylindrical simulation cell is shown in Fig. 1 in an axial cross-section. The protein (excluding the charged atoms of the pore lining, see below) and lipid membrane are represented as hard walls inaccessible to ions (solid lines). Ions are reflected off the surface of these walls and cannot penetrate into the wall itself. A cylindrical hole through the protein (radius  $R_f$ , length  $H_f$ ) connects two reservoirs (baths) that contain mobile ions such as  $\text{Na}^+$ ,  $\text{K}^+$ ,  $\text{Ca}^{2+}$ , and  $\text{Cl}^-$ . The dimensions assigned to the cylindrical hole ( $R_f = 0.4\text{--}0.5\text{ nm}$ ,  $H_f = 1\text{ nm}$ ) represent the narrowest part of the biological channel (the 'selectivity filter'). The baths in this simulation represent both the actual baths around the protein and the wider portions of the channel. Earlier simulations of a Ca channel showed that the inclusion of atria at either end of the pore has only small effects on ion accumulation in the filter.<sup>19</sup> The reflecting radial boundary of the simulation cell is far enough from the channel ( $R = 6.25\text{ nm}$ ) so that edge effects can be neglected, and the axial length of the cell ( $H \approx 25\text{ nm}$ ) is sufficient to allow ionic densities to attain bulk values. Periodic boundary conditions (pbc) are used in the axial direction, making the two baths regions of a single bath.

The filter region of the Na channel contains the side chains of the DEKA locus. Two of these residues (glutamate and aspartate) carry a negatively charged carboxylate group, one residue carries a positively charged amino group (lysine), and one residue (alanine) is electrically neutral. These groups

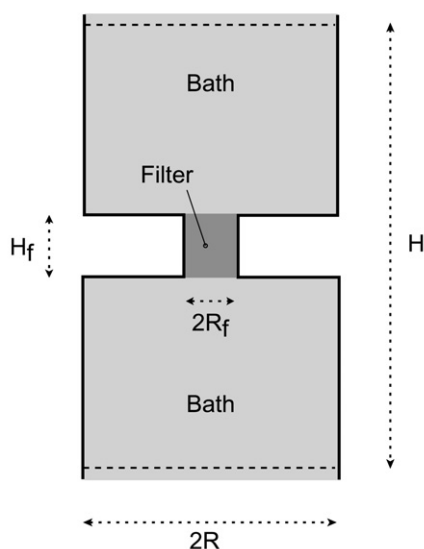


**Fig. 1** Schematic diagram of the simulation cell. Ions are excluded from the membrane (including the channel protein) but not from the bath and channel. Dimensions are specified in the text.

form the ends of side chains and thus are likely to have some mobility. We model these groups as 'dissolved' particles that move without restriction within the filter volume, as do mobile ions (like  $\text{Na}^+$  or  $\text{Ca}^{2+}$ ), but are confined to that volume by structural constraints (not yet specified in physical detail), following earlier work on the EEEE locus.<sup>15-19</sup> Note that in this description the 'filter volume' includes atoms that are part of the channel protein, *i.e.*, atoms that are covalently linked to the protein that makes the channel wall. Specifically, the two carboxylate groups are represented as four 'dissolved' half-charged oxygen ions (hard spheres of diameter 0.28 nm), the amino group is represented as a 'dissolved' ammonium ion (diameter 0.3 nm). The uncharged and short alanine residue is not represented in the model. The centers of the oxygen and ammonium ions are restricted to a subvolume of the filter so they cannot protrude from the filter. Simulations were made with the center of the ammonium ion restricted to the central 0.75 or 0.25 nm of the filter while the oxygen ions were restricted to the central 0.75 nm in all simulations.

The mobile ions are modeled as charged hard spheres with diameters 0.12 nm ( $\text{Li}^+$ ), 0.19 nm ( $\text{Na}^+$ ), 0.266 nm ( $\text{K}^+$ ), 0.34 nm ( $\text{Cs}^+$ ), 0.198 nm ( $\text{Ca}^{2+}$ ), and 0.362 nm ( $\text{Cl}^-$ ). The solvent is represented as a dielectric continuum (dielectric coefficient 78.5) in this so-called primitive model of electrolytes (PM). Nonner *et al.*<sup>15,16</sup> have used both the PM and the solvent primitive model (SPM, in which water is a solvent made of uncharged hard spheres) in computations of the Ca channel and found that the two models give qualitatively similar but quantitatively different predictions of ion accumulation (the SPM gives the same selectivities but in a smaller filter volume). A similar conclusion can be drawn from the works of Tang *et al.* who studied diffusivity and conductivity in a pore using both the PM<sup>22</sup> and the SPM<sup>23</sup> to represent the electrolyte. We start with the PM because its simulations take much less time, allowing much more exploration of conditions and alternatives.

The dielectric coefficient is assumed to be uniform everywhere (78.5) although polarization is likely to be less in the protein or lipid than it is in the aqueous baths. The assumption of a uniform dielectric coefficient is expected to reduce electrostatic effects in the filter. We accept this simplification temporarily because the polarizability of the filter region is presently unknown.

For the details of the canonical MC simulations the reader is referred to reference 19. The electrostatic effect of the periodic images in the axial direction (for which pbc's are applied) was taken into account using the charged line method.<sup>17</sup> The accuracy of this pbc method has been assessed.<sup>24</sup> An important feature of the simulation was that equilibration between the small and crowded filter and the large and dilute bath was accelerated by 'preference sampling'. In this technique, special MC steps, namely particle jumps, are performed, and the jumps that occur between the filter and the bath are given preference. The resulting bias is balanced by a factor that scales the probability of acceptance of MC steps.<sup>19</sup> This method has been calibrated and checked and does not introduce significant error in the domain in which we use it. Because the canonical ensemble was used, bath concentrations were an output of the simulation. Each production run was preceded by a short simulation to obtain an estimate of concentrations, followed by an adjustment of the dimension  $H$  in order to approximate the desired concentrations in the far bath. A typical run consisted of  $3 \times 10^5$  Monte Carlo steps. Error bars shown in Figs. 2, 4, and 6 (below) give the standard errors between local averages formed about subsets of  $10^4$  successive steps.

## 3 Results and discussion

Ca channels contain only carboxylate groups in their selectivity locus and they strongly prefer  $\text{Ca}^{2+}$  over  $\text{Na}^+$  under

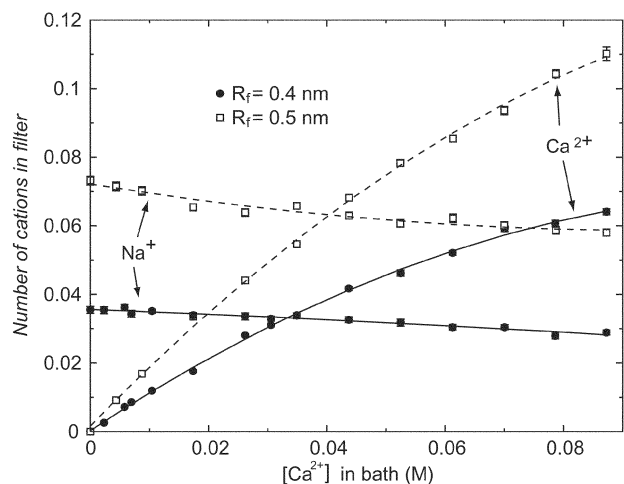


**Fig. 2** Numbers of  $\text{Na}^+$  and  $\text{Ca}^{2+}$  absorbed in the channel volume from a bath containing 0.1 M NaCl and the concentrations of  $\text{CaCl}_2$  indicated on the abscissa. Simulation results (symbols) shown for two filter radii  $R_f$ . The lines are the fit used in refs. 17 and 18 and are meant only to aid the reader in connecting the symbols. The number of ions was determined by integrating ionic concentrations in the region of the filter and a 'cap' at each channel mouth that had radius  $R_f$  and extended one ionic radius in the axial direction of the bath. Note that many error bars are smaller than the symbols. The structural charge in the filter was  $-e$  in all computations.

physiological ionic conditions, in which solutions contain much more  $\text{Na}^+$  than  $\text{Ca}^{2+}$ . Mutated Na channels containing only carboxylate groups also prefer  $\text{Ca}^{2+}$ . Normal Na channels contain a lysine in their selectivity locus and chiefly conduct  $\text{Na}^+$  in physiological conditions (extracellular concentrations  $[\text{Ca}^{2+}] \approx 10^{-3}$  M;  $[\text{Na}^+] \approx 0.1$  M).

We study the effect of the positively charged group (representing lysine) that is present in Na channels but not Ca channels. In the simulations shown in Fig. 2,  $\text{CaCl}_2$  is added to a 0.1 M NaCl bath solution. Results are shown for  $R_f = 0.4$  nm and  $R_f = 0.5$  nm. The total number of ions in the channel is substantially smaller than one (Fig. 2). This number of ions was obtained by integrating average ionic densities over the region defined by  $R_f$  and  $H_f$  plus a 'cap' at each pore mouth that extended by one ionic radius in the axial direction into the bath. With either pore radius, the model of the wild type—*i.e.*, of the natural, *not* mutated—Na channel preferentially absorbs  $\text{Na}^+$  when the  $\text{Ca}^{2+}$  concentration in the bath is near the physiological value (0.001 M). More  $\text{Ca}^{2+}$  than  $\text{Na}^+$  is accepted into the filter only when the concentration of  $\text{Ca}^{2+}$  in the bath is made greater than 30–40 mM. Indeed, if we compare this result to previous work,<sup>15–19</sup> we conclude that our model of the Na channel is a low quality Ca channel.

Ignoring mobile ions, the net charge in the Na channel filter is  $-1$ . Therefore, one might *a priori* expect  $\text{Ca}^{2+}$  to be excluded lest it introduce an excess positive charge and violate local electroneutrality. In a system in which the dielectric coefficient in the membrane protein and filter is less than that the value of 78.5 assumed here, one expects the  $\text{Ca}^{2+}$  to be absorbed even less, because less polarization charge would be present to screen the divalent cation.<sup>25,26</sup> However, Na channels in which the DEKA locus is mutated to DAAA, AEAA, or AAEA, are known to conduct  $\text{Ca}^{2+}$  ion.<sup>11,12</sup> The filter of these mutated channels contains a single negative net charge like the wild type channel that we model. The experimental finding of  $\text{Ca}^{2+}$  conduction in a channel containing a single negative charge indicates that charge neutrality is not strictly preserved within the selectivity locus of real or mutated Na channels. Properties of the channel other than net charge seem to be important for reducing  $\text{Ca}^{2+}$  access.

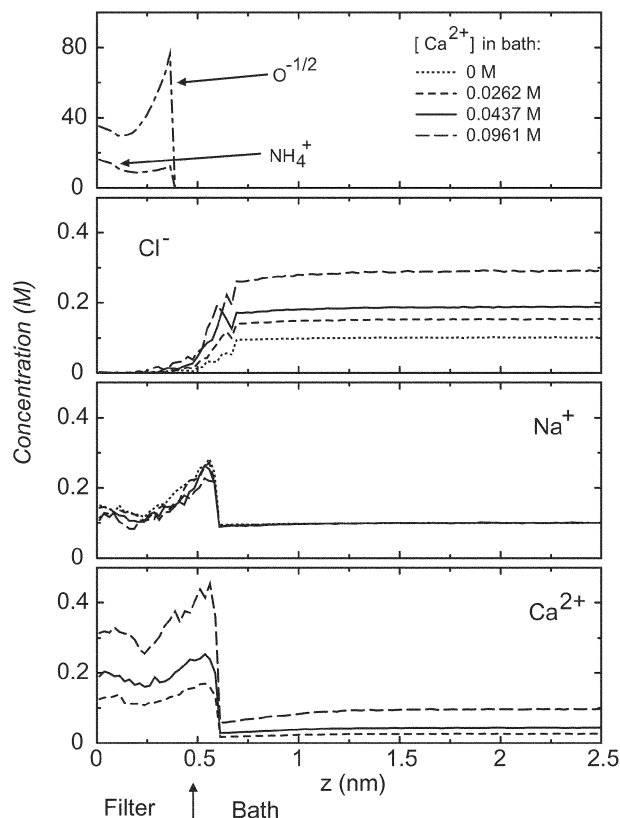


**Fig. 3** Axial concentration profiles. The ordinate gives concentrations averaged over the radial coordinate  $0 \leq r \leq R_f$  (channel) and  $0 \leq r \leq R - R_{\text{ion}}$  (bath), in units of  $\text{mol L}^{-1}$ . The volume accessible to the ion centers was used for the denominator. Note that the abscissa  $z = 0$  corresponds to the center of the simulation cell and channel; the profiles shown are averages of both the left and right half of the symmetrical simulation cell. The arrow marks the position of the mouth of the filter.

One such factor might be the spatial arrangement of positive and negative groups in the locus, *i.e.* some details of the atomic structure of the channel. The locations of the sidechains of the DEKA locus are unknown and so, in our model, we allow the charged groups of the sidechains be anywhere in the filter. Fig. 3 shows the profiles of axial concentration plotted for the channel of Fig. 2 with width  $R_f = 0.4$  nm. Note that the four  $\text{O}^{-1/2}$  ions find their way to the two ends of the filter (the figure plots only the right-hand half of the simulation cell because of the symmetry about the center). We emphasize that this is a *spontaneous nonuniform* arrangement of the tethered ions (*not* imposed by structural constraints from the protein). The distribution of the single positive structural ion—the tethered  $\text{NH}_4^+$ —is much more uniform than the distribution of the structural anions, the tethered  $\text{O}^{-1/2}$  ions.

The spontaneous nonuniform spatial arrangement of tethered charges has important effects on the distributions of mobile species, *e.g.*,  $\text{Na}^+$  and  $\text{Ca}^{2+}$  and is responsible for some of the differences between Ca and Na channels. In the EEEE locus of the Ca channel,  $\text{Na}^+$  and  $\text{Ca}^{2+}$  accumulate in the center of the filter. In the DEKA locus of the Na channel, mobile ions are excluded from the center of the filter and are present in much smaller density altogether. In fact,  $\text{Na}^+$ , the native ion of this channel—which is responsible for the biological function of the wild type  $\text{Na}^+$  channel—has nearly the same density in the bath and filter, although it is somewhat more concentrated in the baths just outside the filter.

The distribution of  $\text{Na}^+$  is consistent with earlier models of Na permeation and with several types of experiments. For instance, the biological channel is known<sup>27–29</sup> to maintain

substantial conductance even when the baths are diluted to less than 1 mM NaCl, as if  $\text{Na}^+$  density near the channel were buffered by a negative surface charge at the channel mouths. Unidirectional tracer fluxes in Na channels indicate that there is no significant correlation among the passages of individual  $\text{Na}^+$  ions,<sup>30,31</sup> as if the (mean time averaged) density of  $\text{Na}^+$  in the channel were not very large (corresponding to less than one ion present on average). Our model gives a distribution of  $\text{Na}^+$  rather like that in chemical kinetic models that have two weak 'binding sites' flanking an activation barrier.<sup>29,32,33</sup>

Our simulations give this distribution of structural charge as a result, not as an assumption. The simulations show that the energetically most favorable distribution of structural charge in the DEKA locus implies a distribution of  $\text{Na}^+$  like that found when two weak binding sites flank a barrier. On the other hand, the density of  $\text{Na}^+$  in the center of the filter in our simulation turns out to be similar to the density of  $\text{Na}^+$  in the bath, so an energy 'barrier' in the sense of transition state theory does not exist for the native ion that carries large currents in the physiological situation. Some workers have doubted that a channel designed to conduct maximal currents would contain large energy barriers.<sup>34</sup>

Although the location of the  $\text{O}^{-1/2}$  ions in the computation reported in Fig. 3 seems reasonable and consistent with experiment, we were interested in studying the effects of confining  $\text{NH}_4^+$  to a smaller region in the center of the filter. Such confinement to the center might produce an electropositive potential barrier in the center of the filter and thus enhance selectivity. Fig. 4 examines the  $\text{Na}^+/\text{Ca}^{2+}$  selectivity of such a channel, with the  $\text{NH}_4^+$  more tightly tethered. Here, we shortened the  $\text{NH}_4^+$  confinement region from a length of 0.375 nm on either side of the channel center to a length of 0.125 nm while  $R_f = 0.4$  nm. Forcing the  $\text{NH}_4^+$  to the center of the filter reduces the absolute selectivity (*i.e.*, the apparent affinity) of the filter region for  $\text{Na}^+$ , but it increases the relative selectivity because it reduces the absolute selectivity of  $\text{Ca}^{2+}$  more so. That is to say, the channel has become an even less efficient Ca channel and more of a Na channel. Density profiles for the constricted  $\text{NH}_4^+$  case are shown in Fig. 5.

### Calcium block of sodium current

In biological Na channels, raising the (extracellular) concentration of  $\text{Ca}^{2+}$ , substantially reduces the  $\text{Na}^+$  current flowing

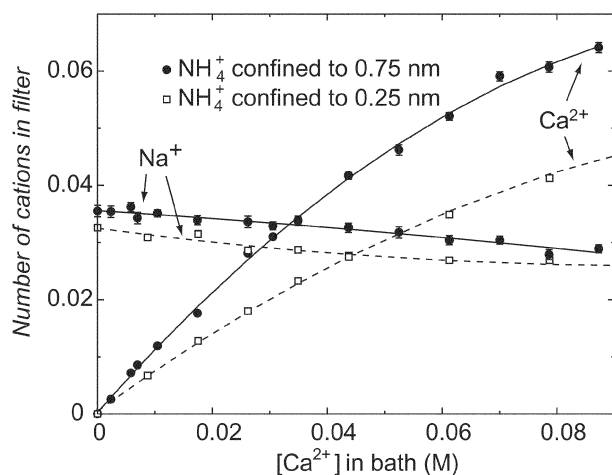


**Fig. 4** Selectivity of a Na channel using a model with  $R_f = 0.4$  nm and  $H_f = 1$  nm for different  $\text{NH}_4^+$  confinements. In the two sets of simulations, the  $\text{NH}_4^+$  ion center is confined to a length of 0.375 nm and 0.125 nm on either side of the channel center, and the structural charge in the filter is  $-1e$ . The symbols give the simulation results (the lines are meant only to aid the reader in connecting the symbols).

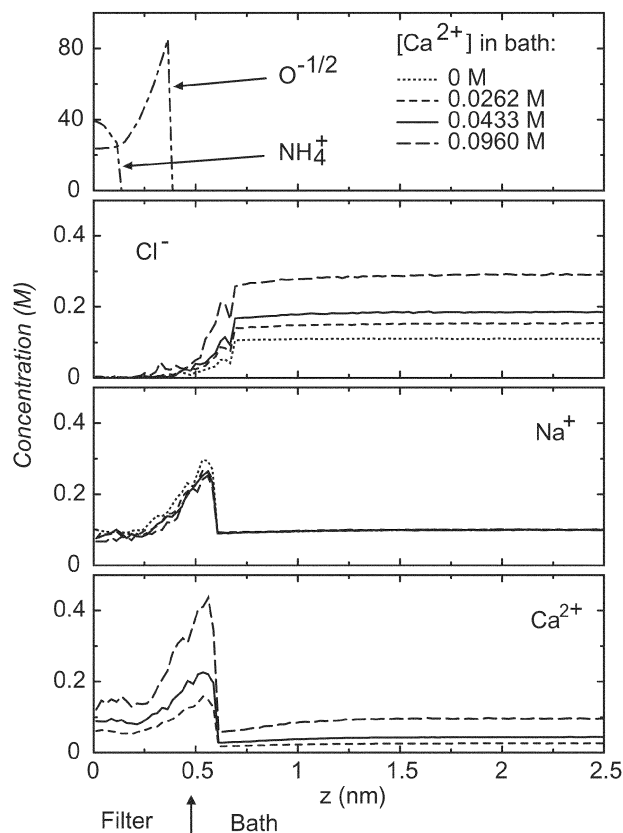


**Fig. 5** Axial concentration profiles obtained with the Na channel model in which the  $\text{NH}_4^+$  ion center is confined to a length of 0.125 nm on either side of the channel center. Profiles are computed as described in Fig. 3.

into the cell (see 35 and references therein). If the density of  $\text{Ca}^{2+}$  in the filter were found to be raised when  $\text{Ca}^{2+}$  is raised in the bath, and the density of  $\text{Na}^+$  in the filter were found to be concomitantly reduced, the current of  $\text{Na}^+$  would be reduced.

Such depletion of  $\text{Na}^+$  by  $\text{Ca}^{2+}$  is not seen in our model, when  $[\text{Ca}^{2+}]$  is raised in the bath: as  $\text{Ca}^{2+}$  is added, more  $\text{Ca}^{2+}$  is accepted into the pore but only small amounts of  $\text{Na}^+$  are removed from the filter (Fig. 2). Furthermore, the overall small (average) densities in the filter imply a small probability for a  $\text{Ca}^{2+}$  and a  $\text{Na}^+$  to meet each other (in the filter). The positively charged group in the model of the DEKA locus reduces  $\text{Ca}^{2+}$  affinity thus preventing  $\text{Ca}^{2+}$  from displacing  $\text{Na}^+$ . Our (self-consistent) calculation suggests that a different explanation of the  $\text{Ca}^{2+}$  block of  $\text{Na}^+$  channels needs to be considered, one that may extend beyond the domain of our model considered here. For instance,  $\text{Na}^+$  might be displaced by  $\text{Ca}^{2+}$  from a region outside the selectivity filter. If an electrochemical gradient were applied across such a channel, the depletion of  $\text{Na}^+$  from a region outside the filter could propagate into the filter and thereby reduce the flux of ions. Nonequilibrium computations are needed to examine this possibility.

### Anion-cation selectivity

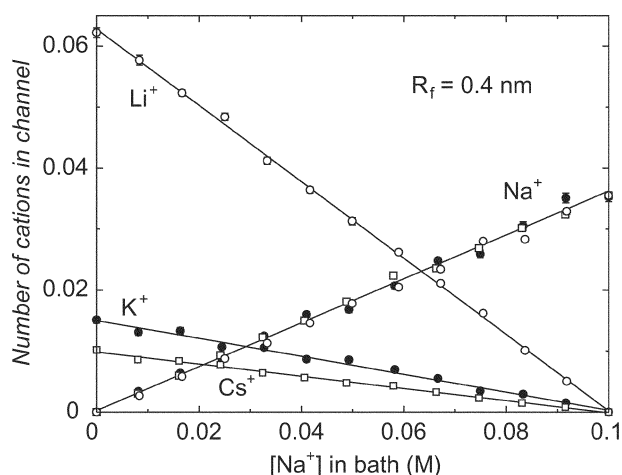
The model of the filter excludes the anion,  $\text{Cl}^-$ , regardless of whether the  $\text{NH}_4^+$  are restricted to the central 0.75 or 0.25 nm of the filter (Figs. 3 and 5). The central region of the filter actually contains net positive structural charge in the restricted case, even though this is a cation channel.  $\text{Cl}^-$ , however, is excluded throughout the filter, even in the positive central region of the restricted case; the forces arising from the

excluded volume of  $\text{Cl}^-$  are large enough, due to the diameter of  $\text{Cl}^-$  (0.362 nm), to overwhelm the electrical forces.

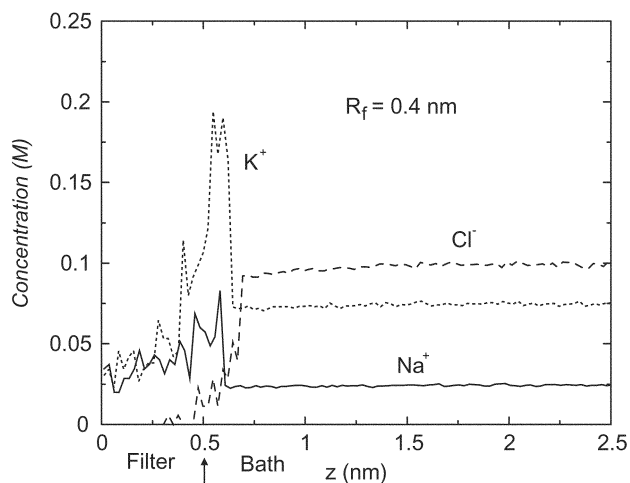
### Selectivity among monovalent cations

Fig. 6 shows selectivity among monovalent cations by plotting the number of  $\text{Li}^+$ ,  $\text{K}^+$ , and  $\text{Cs}^+$  ions absorbed compared to the number of  $\text{Na}^+$  ions absorbed when the  $\text{Na}^+$  channel of radius  $R_f = 0.4$  nm is exposed to mixed solutions. We begin with 0.1 M NaCl and gradually replace  $\text{Na}^+$  ions with one of these cations, holding the concentration of  $\text{Cl}^-$  constant. In the equilibration,  $\text{Li}^+$ ,  $\text{K}^+$ , and  $\text{Cs}^+$  ions replace  $\text{Na}^+$  ions in the bath as well as in the filter. Selectivity is determined by observing which species predominates in the filter when the test cation concentration equals that of  $\text{Na}^+$  in the bath, *i.e.*, at  $[\text{Na}^+] = 0.05$  M. As would be expected from the CSC, the ions of smaller diameter are accepted into the channel selectively in preference to larger ions. Unlike the EEEE locus, this DEKA locus is reluctant to accept a high density of *any* counterion, but smaller alkali metal ions are excluded less than the large ones. The non-physiological ion  $\text{Li}^+$  is preferred over  $\text{Na}^+$ , whereas  $\text{Na}^+$  is preferred over  $\text{K}^+$  or  $\text{Cs}^+$ , as has been observed in experiments.

Fig. 7 plots axial densities of  $\text{Na}^+$  and  $\text{K}^+$  in one simulation in which the bath contained  $\text{Na}^+$  and  $\text{K}^+$  in the ratio  $\approx 1 : 3$ . The distributions of  $\text{K}^+$  and  $\text{Na}^+$  differ from those in the bath. Whereas  $\text{Na}^+$  has similar concentrations in the bath and in the center of the filter,  $\text{K}^+$  is less concentrated in the filter than in the bath;  $\text{K}^+$  has a larger diameter than  $\text{Na}^+$  and thus experiences stronger repulsion from the excluded volume effects that arise in the filter. As a result, the  $\text{K}^+$  ions attracted to the channel mostly dwell just outside the mouths of the channel. Since  $\text{K}^+$  is repelled from the center of the filter,  $\text{K}^+$  is expected to be conducted to a lesser extent than the overall count of  $\text{K}^+$  in and near the filter (Fig. 6) would suggest (a ‘cap’ at each end of the filter is included in the ion count, see legend of Fig. 2).  $\text{K}^+$  conductance could be decreased even more by reducing the volume in which the structural ions are confined. Nevertheless, even when  $\text{K}^+$  is ‘penalized’, significant amounts of  $\text{K}^+$  are absorbed by the channel when the ratio of  $\text{K}^+/\text{Na}^+$  in the bath is made large enough (Fig. 6). Garber and Miller<sup>28</sup> have shown that Na channels conduct  $\text{K}^+$  under such ionic conditions: when  $\text{Na}^+$  is removed altogether from the baths,



**Fig. 6** Selectivity of  $\text{Li}^+$ ,  $\text{K}^+$ , and  $\text{Cs}^+$  vs.  $\text{Na}^+$  in a Na channel. The filter radius in the model is  $R_f = 0.4$  nm, and the  $\text{NH}_4^+$  is restricted to the central 0.75 nm of the filter. The structural charge in the filter is  $-1e$ . In these simulations we start with a 0.1 M NaCl solution in the bath and gradually replace the  $\text{Na}^+$  ions with different cations, holding the concentration of  $\text{Cl}^-$  constant at 0.1 M. The straight lines are meant only to aid the reader in connecting the points.



**Fig. 7** Axial concentration profiles of the Na channel model with  $R_f = 0.4$  nm. In this simulation, the bath contained a 0.1 M mixture of NaCl and KCl in the ratio  $\approx 1:3$ . Profiles are computed as described in Fig. 3.

the filter of the model Na channel will accept other cations due to the electrostatic force.

### Dielectric coefficient

Our simulations use a uniform dielectric coefficient everywhere, which is that of bulk water (78.5). If a smaller dielectric coefficient were applied to the filter and/or protein, the need for charge balance within the filter itself would be greater, and so a larger density of counterion would be found in the filter itself. Given the intrinsic charge of  $-1$  of the DEKA locus, the countercharge should more closely approach  $+1$  if the dielectric coefficient is reduced. On the other hand, ions entering a filter with reduced dielectric coefficient might have to be desolvated to some degree, and that would reduce entry into the filter. If the counterion density were larger than that in our simulations, as the net effect of a reduction in dielectric coefficient, excluded volume effects would be stronger. Thus, a channel with a (spatially) uniform reduced dielectric coefficient is expected to exclude large ions more strongly than the channel with the uniformly large dielectric coefficient.

### Experimental measures of selectivity

Most experimental assessments of  $\text{Na}^+/\text{K}^+$  selectivity are based on measurements of the zero-current potential in bi-ionic conditions, when one cation species is present in only one bath, and the other species is present only in the other bath. Typically, a permeability ratio  $\approx 10 : 1$  has been found (reviewed in ref. 1), reflecting both equilibrium binding and frictional factors of permeation.<sup>36</sup> Selectivity has also been estimated from measurements of current made by varying the mole fractions of  $\text{Na}^+$  and  $\text{K}^+$  in both baths, while keeping the total salt concentration constant. This ‘mole fraction experiment’ more directly assesses the partitioning factor of selectivity.<sup>36</sup> Ravindran *et al.*<sup>35</sup> found that current in batrachotoxin treated Na channels is reduced by about one-half when  $\text{Na}^+$  and  $\text{K}^+$  mole fractions are equal, which suggests that partitioning is not the only determinant of selectivity in the Na channel. However, all these experiments are clearly performed away from equilibrium, and so quantitative predictions of their results require non-equilibrium simulations or theory, beyond those reported here. We expect to deal with this issue in the future using density functional theory in a drift/diffusion model of transport.<sup>20</sup> For the time being, we note that the CSC mechanism gives equilibrium ionic affinities that agree

with the order of permeabilities determined from zero-current potentials for alkali metal ions.

### Mechanism of selectivity

Our simulations reveal a simple mechanism for alkali metal selectivity in the Na channel that depends on the crowding of charges in the channel. The mechanism of selectivity in the Na channel is a different twist on the competition between charge and space found in the Ca channel. In the Na channel, the presence of a positively charged lysine residue greatly diminishes affinity for divalent cations.

The structure underlying our proposed mechanism is not the structure that has previously been ascribed to the selectivity filter of the Na<sup>+</sup> channel, in which oxygen atoms (some charged) were said to form the rigid wall of a 0.3 × 0.5 nm wide hole through the protein.<sup>13,14</sup> The latter structure has been widely accepted – it is found in textbooks – but its ability to select Na<sup>+</sup> has, to our knowledge, not been tested in self-consistent computations.

Following Eisenman,<sup>37</sup> Hille proposed that a channel of this structure could use an anionic ‘high field-strength site’ to select small alkali metal ions over larger ones by electrostatics. In contrast to this view, the alkali metal selectivity that we have computed in Monte Carlo simulations arises chiefly from the effects of excluded volume, not from electric field strength. In our calculations, the chief effect of the electric field is to simply attract cations to the filter, where larger ions then are *excluded* more than small ions. By contrast, in the electrostatic hypothesis smaller cations are *attracted* more than larger cations to the structural charges of the filter. The exclusion of K<sup>+</sup> in our model is evident in the density profiles of Fig. 7: K<sup>+</sup> density is minimal (and below bulk density) in the center of the pore. Thus the region of strongest selectivity is where the density of structural net charge is minimal (see densities of O<sup>-1/2</sup> and NH<sub>4</sub><sup>+</sup> in Fig. 3). Recent experiments have shown that Na channels whose DEKA locus is mutated to DAAA, AEAA, or AAEA (*i.e.*, a locus containing a single carboxylate) select for Ca<sup>2+</sup> over Na<sup>+</sup>.<sup>11,12</sup> Thus, creating a ‘high field-strength site’ in the sense of Eisenman yields a Ca channel, not a Na channel. In this context it becomes obvious that Hille’s model of the selectivity filter lined only by negative or polar oxygens never adequately explained how the channel excludes Ca<sup>2+</sup>.

Goulding *et al.*<sup>(38,39)</sup> have used density functional theory and simulations to study ‘entropic selectivity of microporous materials.’ They specifically examine absorption into a hard-wall pore of an uncharged hard-sphere fluid made of a solvent and two solutes, with diameters corresponding to water, Na<sup>+</sup> and K<sup>+</sup>. The results reveal selective *excess absorption* of one of the solutes over the other depending on certain small ratios of pore and particle diameters. Little selectivity is observed for the diameter we assign to the Na channel ( $R_f/R_{Na} \approx 4$ ). On the other hand, our simulations indicate substantial excluded-volume selectivity that is *repulsive* (small ions are repelled less than large ions) under these conditions. Our simulations differ from those of Goulding *et al.* because we include a high density of particle species that are restricted to the pore (the tethered oxygen and nitrogen ions) and we use a non-particulate description of water. Thus, in our model the pore contains a fluid-like density of confined and mobile ions, whereas the bath is represented as an ion gas. The asymmetry in densities is the basis of the observed repulsion of ions from the filter. This repulsion increases monotonically with ionic diameter (Fig. 6), whereas the absorption observed by Goulding *et al.* can select for either smaller or larger ions dependent on small variations of channel diameter.

*Repulsive phenomena as observed in our simulations can in principle occur in two bulk phases of different particle densities and do not require a particular wall structure or channel*

*diameter.* In fact, Nonner *et al.*<sup>15,16</sup> have studied bulk models of a Ca channel and assessed entropic repulsive effects. In these models, water can be conveniently described in both the particulate and non-particulate models, so it is possible to assess the role of a particulate solvent. It was found that comparable repulsive selectivities can arise from excluded volume effects when appropriate filter volumes are chosen for either model: if water is described as particulate, a smaller filter volume is needed. In this case of particulate water, the confined particles in the filter are more compressed compared to calculations with non-particulate water. In both cases, there exists an asymmetry of density between the filter and bath fluids. Thus, we expect that the repulsive selectivity observed in our simulations of the Na channel would occur also when water is described as particulate, if an appropriate reduction is made to the filter volume.

It is also interesting to consider the consequences if water itself were attracted or repelled into or out of the selectivity filter. In the case of attraction, water would compete more strongly with ions for the space in the filter, and so the selective effects of excluded volume would be enhanced. If water were repelled from the filter, less repulsive selectivity would be expected. Again, (experimentally) appropriate selectivities could be produced by adjusting the volume of the filter of the model.

Our simulations were made using a specific representation of charged tethered groups and a particular estimate of the volume accessible to these groups but the simulations do not hinge on these choices. For instance, we could have represented larger parts of the DEKA sidechains by including neutral confined particles in the simulation, and increased the volume in which these groups are confined. Specifically, the relatively bulky sidechain of lysine could be modeled more realistically this way.<sup>12</sup>

*The crucial parameter for a CSC mechanism as described here is the packing fraction of the ensemble of all atoms, mobile and structural, in the filter.* The crowding of ions and protein atoms allow the finite size of the ions to determine selectivity. The mechanism does not require a specific geometry in which atomic positions and dimensions are strictly maintained.

## 4 Conclusions

Ion absorption has been computed for a model of the DEKA locus of biological Na channels in which mobile ions and charged structural groups are represented as charged hard spheres. The model channel selects Na<sup>+</sup> essentially by *excluding* larger monovalent cations while having a relatively weak affinity for Ca<sup>2+</sup>. The presence of the positively charged lysine residue in the locus is essential for making the Na channel a ‘reluctant’ Ca channel. Excluded volume effects are essential for selecting small monovalent cations over large ones (CSC mechanism).

## Acknowledgements

This work was supported by grants from the Hungarian National Research Fund (OTKA-F035222, to D.B.), DARPA (B.E., W.N.), NIH (AI 23007, to D.D.B.), and NSF (CHE98-13729, to D.H.). The authors thank Dr D. Gillespie for many useful comments and to Dr R. F. Rakowski for sharing results submitted for publication.

## References

- 1 B. Hille, *Ionic Channels of Excitable Membranes*, Sinauer Associates, Inc., Sunderland, MA, 2001.
- 2 F. M. Ashcroft, *Ion Channels and Disease*, Academic Press, New York, 1999.

- 3 A. L. Hodgkin and A. F. Huxley, *J. Physiol. (London)*, 1952, **117**, 500.
- 4 D. A. Doyle, J. M. Cabral, R. A. Pfuetzner, A. Kuo, J. M. Gulbis, S. L. Cohen, B. T. Chait and R. MacKinnon, *Science*, 1998, **280**, 69.
- 5 H. R. Guy and S. R. Durell, in *Ion Channels and Genetic Diseases*, ed. D. Dawson, Rockefeller University Press, New York, 1995, pp. 1–16.
- 6 H. Terlau, S. H. Heinemann, W. Stühmer, M. Pusch, F. Conti, K. Imoto and S. Numa, *FEBS Lett.*, 1991, **293**, 12.
- 7 J. Yang, P. T. Ellinor, W. A. Sather, J.-F. Zhang and R. W. Tsien, *Nature*, 1993, **366**, 158.
- 8 R. G. Tsushima, R. A. Li and P. H. Backx, *J. Gen. Physiol.*, 1997, **109**, 463.
- 9 M. T. Perez-Garcia, N. Chiamvimonvat, R. Ranjan, J. R. Balsler, G. F. Tomaselli and E. Marban, *Biophys. J.*, 1997, **72**, 989.
- 10 S. H. Heinemann, H. Terlau, W. Stühmer, K. Imoto and S. Numa, *Nature*, 1992, **356**, 441.
- 11 I. Favre, E. Moczydlowski and L. Schild, *Biophys. J.*, 1996, **71**, 3110.
- 12 Y.-M. Sun, I. Favre, L. Schild and E. Moczydlowski, *J. Gen. Physiol.*, 1997, **110**, 693.
- 13 B. Hille, *J. Gen. Physiol.*, 1971, **58**, 599.
- 14 B. Hille, *J. Gen. Physiol.*, 1972, **59**, 637.
- 15 W. Nonner, L. Catacuzzeno and B. Eisenberg, *Biophys. J.*, 2000, **79**, 1976.
- 16 W. Nonner, D. Gillespie, D. Henderson and B. Eisenberg, *J. Phys. Chem. B*, 2001, **105**, 6427.
- 17 D. Boda, D. D. Busath, D. Henderson and S. Sokolowski, *J. Phys. Chem. B*, 2000, **104**, 8903.
- 18 D. Boda, D. Henderson and D. D. Busath, *J. Phys. Chem. B*, 2001, **105**, 11 574.
- 19 D. Boda, D. Henderson and D. D. Busath, *Mol. Phys.*, 2002, **100**, 2361.
- 20 D. Gillespie, W. Nonner and R. S. Eisenberg, *J. Phys.: Condens. Matter*, 2002, in press.
- 21 J. G. M. Barthel, H. Krienke and W. Kunz, *Physical Chemistry of Electrolyte Solutions. Modern Aspects*, Steinkopff, Darmstadt, Springer, New York, 1998.
- 22 Y.-W. Tang, I. Szalai and K.-Y. Chan, *Mol. Phys.*, 2001, **99**, 309.
- 23 Y.-W. Tang, I. Szalai and K.-Y. Chan, *J. Phys. Chem. A*, 2001, **105**, 9616.
- 24 Y. Yang, D. Henderson, P. Crozier, R. L. Rowley and D. D. Busath, *Mol. Phys.*, 2002, **100**, 3011.
- 25 G. Moy, B. Corry, S. Kuyucak and S.-H. Chung, *Biophys. J.*, 2000, **78**, 2349.
- 26 B. Corry, S. Kuyucak and S.-H. Chung, *Biophys. J.*, 2000, **78**, 2364.
- 27 W. N. Green, L. B. Weiss and O. S. Andersen, *J. Gen. Physiol.*, 1987, **89**, 841.
- 28 S. S. Garber and C. Miller, *J. Gen. Physiol.*, 1987, **89**, 459.
- 29 D. Naranjo and R. Latorre, *Biophys. J.*, 1993, **64**, 1038.
- 30 T. Begenesich and D. D. Busath, *J. Gen. Physiol.*, 1981, **77**, 489.
- 31 R. F. Rakowski, D. C. Gadsby and P. De Weer, *J. Gen. Physiol.*, 2002, **119**, 235.
- 32 B. Hille, *J. Gen. Physiol.*, 1975, **66**, 535.
- 33 A. Ravindran, H. Kwiecinski, O. Alvarez, G. Eisenman and E. Moczydlowski, *Biophys. J.*, 1992, **61**, 494.
- 34 D. Chen, L. Xu, G. Tripathy, G. Meissner and R. Eisenberg, *Biophys. J.*, 1997, **73**, 1337.
- 35 A. Ravindran, L. Schild and E. Moczydlowski, *J. Gen. Physiol.*, 1991, **97**, 89.
- 36 D. Gillespie and R. S. Eisenberg, *Eur. Biophys. J.*, 2002, in press: DOI 10.1007/s00249-002-0239-x.
- 37 G. Eisenman, in *Ion-Selective Electrodes*, NBS Spec. Pub. 314, ed. R. A. Durst, National Bureau of Standards, Gaithersburg, MD, p. 1.
- 38 D. Goulding, J.-P. Hansen and S. Melchionna, *Phys. Rev. Lett.*, 2000, **85**, 1132.
- 39 D. Goulding, J.-P. Hansen and S. Melchionna, *Phys. Chem. Chem. Phys.*, 2001, **3**, 1644.